Range of shortcuts in the dynamic model of neural networks

2010 J. Phys. A: Math. Theor. 43 205001

(http://iopscience.iop.org/1751-8121/43/20/205001)

J. Phys. A: Math. Theor. **43** (2010) 205001 (11pp) doi:10.1088/1751-8113/43/20/205001

Range of shortcuts in the dynamic model of neural networks

J Choi[1], M Y Choi[2], M S Chung[3] and B-G Yoon[3,4,5]

[1] Department of Physics and Department of Chemical Engineering, Keimyung University, Daegu 704-701, Korea
[2] Department of Physics and Astronomy and Center for Theoretical Physics, Seoul National University, Seoul 151-747, Korea
[3] Department of Physics, University of Ulsan, Ulsan 680-749, Korea
[4] Research Center for Dielectric and Advanced Material Physics, Pusan National University, Busan 609-735, Korea

E-mail: bgyoon@ulsan.ac.kr

Received 16 July 2009, in final form 26 March 2010
Published 30 April 2010
Online at stacks.iop.org/JPhysA/43/205001

Abstract
We study, via extensive Monte Carlo calculations, the effects of the range of shortcuts in the dynamic model of neural networks. With the increase of the range of shortcuts, the Mattis-state order parameter grows and the ordered-state region expands in the phase diagram, encroaching upon the mixed-phase region in the phase diagram. In particular, the power spectra of the order parameter at stationarity are observed to exhibit different shapes, depending on the range of shortcuts in the network. The cluster size distribution of the memory-unmatched sites, as well as the distribution of waiting times for neuron firing, possesses strong correlations with the power spectra in their shapes, all exhibiting the most pronounced power-law behaviors when the range of shortcuts is long.

PACS numbers: 05.65.+b, 87.18.Bb, 87.18.Sn

(Some figures in this article are in colour only in the electronic version)

1. Introduction

Typical properties exhibited by complex networks are related with the so-called small-world topology [1], characterized by clustering and short path length, as well as power-law-type scaling. The brain provides one of the best-known systems exhibiting small-world topology, anatomically and functionally [2]; there is experimental evidence for the human brain that some regions of the nervous system, e.g., the visual cortex, possess small-world geometry [3, 4]. It is well known that neural networks in small-world topology have some advantages: retrieval

[5] Author to whom correspondence should be addressed.

performance is enhanced, compared to those in random-network topology with the same total connection length [5]. In general, the connection topology is expected to affect substantially the dynamics of the system. Nevertheless there are few works addressing dynamics of the neural network on the small-world geometry [6].

In a recent work, we have investigated the dynamic model of neural networks on the small-world geometry, varying the connectivity of neurons [7]. Through the use of Monte Carlo (MC) calculations the model has been shown to exhibit many desirable properties. For example, the order parameter in general grows with the number of connections. In particular, the power spectrum has correlations with the cluster-size distribution of 'memory-unmatched neurons'; both exhibit power-law behaviors, which are more pronounced with the increase of the connectivity. The waiting time, i.e. the time elapse for a neuron to wait for the next firing, has also been considered and its distribution has been found to follow roughly a power law, which is consistent with findings in brain activity: namely, electroencephalogram displays $1/f$ frequency scaling [8] and waiting times (interspike intervals) in cortex neurons follow a power-law distribution [9]. One notable thing in MC calculations is that the shape of power-law behavior is dependent upon how the connectivity is varied, e.g. there appear inflection points in the power spectrum and in the cluster-size distribution only in the case of increasing the number of coupled neurons with relatively short correlation lengths. It is thus of interest to see how the correlation length affects the small-world neural network.

In this work we further elaborate this point by varying the maximum range of shortcuts, which measures the correlation length in the neural network, and study its effects, focusing on the (global) order parameter and on the dynamic properties of the system. Observed is monotonic growth of the order parameter as the shortcut range (or the correlation length) is increased, together with the retrieval of a mixture of memories, especially for short ranges of shortcuts. The phase diagram of the network is constructed and how it varies with the shortcut range is exposed. We then compute the power spectrum of the order parameter, which displays, for a given value of the order parameter, different shapes depending on the shortcut range. Further, the power spectrum has correlations with the cluster-size distribution of memory-unmatched neurons; both exhibit power-law behaviors, which become more pronounced as the shortcut range is increased. We also consider the waiting time, the distribution of which again exhibits more power-law-like behavior for longer ranges of shortcuts.

This paper consists of five sections. In section 2, the dynamic model of neural networks is briefly reviewed and the method of MC calculations is described. Section 3 presents the results, showing how the phase diagram as well as the order parameter changes with the shortcut range in the network. In section 4, we describe the dependence of the power-law behaviors on the range of shortcuts. Finally, a summary is given in section 5.

2. Dynamic model and Monte Carlo calculations

We consider a network consisting of N neurons, the ith of which is described by an Ising spin $s_i = \pm 1$ according to whether it is firing or not. The threshold behavior of the ith neuron at time t is governed by the probability depending on the local potential

$$E_i' = \sum_j J_{ij} s_j', \tag{1}$$

where $2J_{ij}$ is the strength of the synaptic junction from the jth neuron to the ith one ($J_{ii} \equiv 0$) and s_j' denotes the state of the jth neuron at time $t - t_d$ with t_d being the time delay in interaction (i.e. retardation of signal propagation, mostly through the synaptic junction) [10].

According to the simple Hebb-type learning rule [11], the synaptic strength is constructed of p stored patterns:

$$J_{ij} = \begin{cases} N^{-1} \sum_{\mu=1}^{p} \sigma_i^\mu \sigma_j^\mu & \text{for} \quad i \neq j \\ 0 & \text{for} \quad i = j, \end{cases} \tag{2}$$

where $\sigma_i^\mu = \pm 1$ is the state of the ith neuron in pattern $\mu (=1, 2, \ldots, p)$.[6]

We first prescribe the conditional probability $p(-s_i, t + \delta t | s_i, t; \mathbf{s}', t - t_d)$ that the ith neuron in state s_i at time t changes its state to $-s_i$ at time $t + \delta t$, which manifests the dependence on the configuration of the system, $\mathbf{s}' \equiv (s_1', s_2', \ldots, s_N')$, at time $t - t_d$. In the limit $\delta t \to 0$, the conditional probability can be expressed in terms of the transition rate:

$$p(-s_i, t + \delta t | s_i, t; \mathbf{s}', t - 1) = w_i(s_i; \mathbf{s}', t - 1)\delta t, \tag{3}$$

where time t has been re-scaled in units of the delay time t_d (see reference [10] for details). The transition rate reads

$$w_i(s_i; \mathbf{s}', t - 1) = \frac{1}{2\tau} \left[\left(a + \frac{1}{2} \right) + \left(a - \frac{1}{2} \right) s_i + \frac{1 - s_i}{2} \tanh \beta E_i' \right] \tag{4}$$

with $\tau \equiv t_r / t_d$ and $a \equiv t_r / t_0$, where t_r is the refractory period and t_0 is the time duration of the action potential, usually of the order of one to a few milliseconds. The 'temperature' $T \equiv 1/\beta$ measures the width of the threshold region or the noise level.

The behavior of the network is then governed by the master equation, which describes the evolution of the joint probability $P(\mathbf{s}, t; \mathbf{s}', t - 1)$ that the system is in state $\mathbf{s}'$ at time $t - 1$ and in state $\mathbf{s}$ at time t. In consequence, equations describing the time evolution of relevant physical quantities, with the average taken over $P(\mathbf{s}, t; \mathbf{s}', t - 1)$, in general assume the form of differential-difference equations due to the delay in interactions. For example, one may find the equation of motion for $\langle s_i \rangle_t \equiv \sum_{\mathbf{s}} \sum_{\mathbf{s}'} s_i P(\mathbf{s}, t; \mathbf{s}', t - 1)$, which relates to the activity of the ith neuron via $A_i(t) \equiv (1/2)(1 + \langle s_i \rangle_t)$. In the case of the infinite-range interaction or in the fully connected limit, the equation of motion leads to the self-consistency equation [10]. One may also find the time evolution equation for the 'order parameter' $q^\mu(t) \equiv N^{-1} \sum_i \sigma_i^\mu \langle s_i \rangle_t$, which describes the overlap between the neurons and the memory μ.

In this work, we focus on the Mattis-state solution of the form $q^\mu(t) \equiv q(t)\delta_{\mu 1}$, which is fully correlated with just one of the quenched memories. As usual, patterns are generated at random, i.e. σ_i^μ is taken to be a quenched random variable, assuming $+1$ and -1 with equal probabilities:

$$p(\sigma_i^\mu) = \tfrac{1}{2}\delta(\sigma_i^\mu - 1) + \tfrac{1}{2}\delta(\sigma_i^\mu + 1). \tag{5}$$

To investigate the correlation length effects, we put neurons on a square lattice of linear size L and perform dynamic MC simulations, varying the maximum range of shortcuts in the system. In the beginning, each neuron is coupled to its first and second nearest neighbors, namely the number of primary connections is 8 per neuron. Subsequently, a shortcut is added with given probability between each neuron and another chosen randomly within distance $R_{\max}$, the maximum range of shortcuts, in units of the lattice constant. We then probe the behavior of the system as the shortcut range $R_{\max}$ is varied, together with $N_{\rm sc}$, the total number of shortcuts, varied as well.

In MC calculations, we use the lattice size $L = 64$ and 128 with the number of shortcuts up to $N_{\rm sc} = 43\,300$.[7] We also consider one to four memory patterns ($1 \leqslant p \leqslant 4$), which are

[6] Here we do not consider the asymmetry of synaptic couplings which is present in real neural networks as well as neuronal states other than the two (firing/non-firing).

[7] To disclose the effects of the range of shorcuts on the phase transition and dynamic behavior, we take larger values of $N_{\rm sc}$ compared with conventional small-world networks. Nevertheless, various power-law behaviors as well as a rapid approach to the mean-field limit, characteristics of small-world networks, are observed.

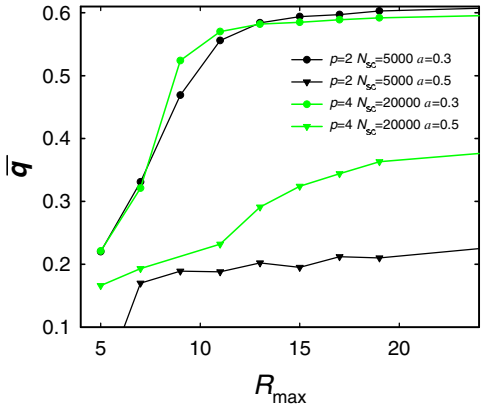

Figure 1. Mattis-state order parameter $\bar{q}$ versus the shortcut range $R_{\max}$. Data have been obtained from MC calculations, for different sets of parameters: $p = 2$, $N_{\rm sc} = 5000$ (black symbols) and $p = 4$, $N_{\rm sc} = 20\,000$ (gray symbols). There are a total of $N = 4096$ neurons at temperature $T = 0.1$, with the time ratio $a = 0.3$ (circles) and 0.5 (triangles). The lines shown are for clarity purposes.

generated according to equation (5) at each run. The initial state of the system is chosen to be one of the memories, which, together with the p memories and given connectivity of the lattice, comprises one configuration. Specifically, we consider 100 different configurations for each set of values (a, T) and set the relaxation time $\tau = 5$ and the time step $\Delta t = 0.5$. These parameter values have been varied, only to give no appreciable difference except for the time scale. Then the neuronal states are allowed to flip according to the transition probabilities in equation (4). To ensure stationarity, we have discarded initial 15 000 (sometimes up to 40 000) time steps before taking time averages of the Mattis-state order parameter $\bar{q}$. The stationary state of a system is either ordered ($\bar{q} \neq 0$) or disordered ($\bar{q} = 0$); the given set of (a, T) belongs to the ordered phase if there exists at least one ordered (Mattis) state with no disordered state, among those states evolved from 100 initial configurations. When there are both disordered states and ordered states, we have the mixed phase. (In the mixed phase, either a Mattis state or a disordered one is retrieved depending on the initial configuration and the time evolution process.) Finally, the phase is considered disordered if there is no Mattis state at all. Note that only the Mattis state (and no other ordered states) is concerned with these criteria.

3. Phase diagrams

We first display in figure 1 the time-averaged Mattis-state order parameter (at stationarity) $\bar{q}$ versus the shortcut range $R_{\max}$, obtained from MC calculations for networks of $N = 4096$ neurons on a square lattice of size $L = 64$ at temperature $T = 0.1$, for (i) $p = 2$, $N_{\rm sc} = 5000$, $a = 0.3$ (black circles); (ii) $p = 4$, $N_{\rm sc} = 5000$, $a = 0.3$ (gray circles); (iii) $p = 2$, $N_{\rm sc} = 20\,000$, $a = 0.5$ (black triangles); (iv) $p = 4$, $N_{\rm sc} = 20\,000$, $a = 0.5$ (gray triangles). For a given set of parameter values, $\bar{q}$ in general grows with $R_{\max}$, implying that a longer correlation length makes the system more effective in memory retrieval for the same number $N_{\rm sc}$ of shortcuts. On the other hand, a larger value of a, with the same values of other parameters, tends to reduce $\bar{q}$, making the system less effective in memory retrieval. With the increase of the number p of memory patterns, the behavior of the order parameter $\bar{q}$

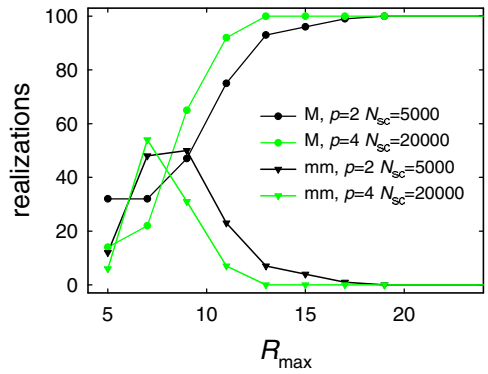

Figure 2. Number of realizations of the Mattis (M) state (circles) and of the multiple-memory (mm) state (triangles) versus the shortcut range $R_{\max}$. Data have been obtained simultaneously with those for $a = 0.3$ in figure 1, from 100 systems with different initial configurations.

remains qualitatively the same, although we need more shortcuts to achieve the same value of $\bar{q}$ (compared with the case of smaller values of p). It is also worthy to mention that $\bar{q}$ seemingly approaches an asymptotic value as $R_{\max}$ is increased.

In the regime where $\bar{q}$ is relatively small, there may emerge another ordered state different from the Mattis state. This state is characterized by mixture of memories, i.e. overlaps with more than one memories, and thus called the multiple-memory state. Figure 2 exhibits the number of realizations of the Mattis state (circles) and of the multiple-memory states (triangles) versus the shortcut range $R_{\max}$ for $a = 0.3$. Data have been obtained simultaneously with those in figure 1, from 100 systems with different initial configurations. As $R_{\max}$ is increased, the number of realizations of the Mattis state as well as the total number of ordered states (including multiple-memory states) increases monotonically. However, the number of multiple-memory states first grows to reach a peak value and then reduces as $R_{\max}$ is increased further, suggesting that such states appear for short correlation lengths.

It is of interest to note that the multiple-memory state is spatially inhomogeneous, so that it retrieves one particular memory pattern in one region and another in the other region of the network. To demonstrate this, we display in figure 3 'memory-unmatched neurons' i.e. those neurons in the state s_i with $s_i\sigma_i^\mu = -1$ (for $\bar{q} > 0$), in the multiple-memory state: such neurons are denoted by black spots for memory patterns (a) $\mu = 1$ and (b) $\mu = 2$. As addressed above, large values of $R_{\max}$ suppress the appearance of these states. We point out, however, that for some set of parameter values, the number of multiple-memory states is saturated (i.e. the decrease in the number is not observed) as $R_{\max}$ is increased. This type of behavior is observed for systems in the mixed phase.

Based on these MC calculations for systems of neurons on a square lattice of $L = 64$, we construct approximate phase diagrams on the plane of the temperature T versus the time ratio a. They are presented in figure 4 with parameters (a) $p = 2$, $N_{\rm sc} = 10\,000$, $R_{\max} = 5$; (b) $p = 2$, $N_{\rm sc} = 10\,000$, $R_{\max} = 15$; (c) $p = 2$, $N_{\rm sc} = 20\,000$, $R_{\max} = 15$; and (d) $p = 4$, $N_{\rm sc} = 20\,000$, $R_{\max} = 15$. Here solid lines describe the boundaries between the mixed phase and disordered one, whereas dashed lines separate the ordered phase from the mixed one. Namely, starting from the disordered phase at high temperatures, the system undergoes transitions to the mixed phase and to the ordered phase at temperatures T_1 and T_2, respectively.

Figure 3. Memory-unmatched sites (black spots) for the memory patterns (*a*) $\mu = 1$ and (*b*) $\mu = 2$ in the multiple-memory state of the system with $p = 2$.

For comparison, the theoretical curves of T_1 and T_2 for the fully connected (mean-field) system, reproduced from reference [10], are also plotted by thick gray lines in (c). Comparing (a) and (b), we find that the region of the ordered phase expands as $R_{\max}$ is increased for given number $N_{\rm sc}$ of shortcuts; this manifests the enhancement of memory retrieval ability with the increase of the correlation length of neurons. Comparison of (a) and (c) also indicates that both T_1 and T_2 get higher, resulting in the expansion of the region of the ordered phase, as $N_{\rm sc}$ is increased for a given value of $R_{\max}$. On the other hand, the ordered-phase region tends to shrink as the number p of memories is increased for given values of $R_{\max}$ and $N_{\rm sc}$, shown in (d). One thing to note is that there always appears the mixed-phase region regardless of the value of a, when the number of connections or $N_{\rm sc}$ is finite. This contrasts with the fully connected network, for which this region exists only for small values of a below the critical value a_c [10].

4. Power-law behaviors

In this section, we present how the power-law behaviors change, as the connectivity, particularly, the shortcut range $R_{\max}$, is varied. Figure 5 displays a series of power spectrum $P(\omega)$ of the order parameter versus frequency $\omega/2\pi$ in a network of neurons on a square lattice of size $L = 128$, resulting from the stationary MC time series of the order parameter $q(t)$. Each set of data has been obtained for the same time ratio $a = 0.3$ at temperature $T = 0.1$. The values of $R_{\max}$ and $N_{\rm sc}$, shown in the legend, have been chosen to give the same value of the Mattis-state order parameter, given by: (a) $\bar{q} = 0.25$, (b) $\bar{q} = 0.45$, and (c) $\bar{q} = 0.65$. It is observed in figure 5(*a*), which belongs to the mixed phase, that the power spectra exhibit apparently power-law behavior: $P(\omega) \propto \omega^{-\gamma}$ with the exponent $\gamma = 1.7$ (see the straight line) over a wide range of the frequency $\omega/2\pi$. In the mixed phase, the state of the system is marginal between order and disorder, with very small values of the order parameter; this is reminiscent of the critical region in a commonly observed phase transition. It is thus not surprising to observe the power-law behavior. We still observe power-law behavior of $P(\omega)$ for larger values of the order parameter, as shown in figures 5(*b*) and (*c*), both of which belong to the ordered-phase region in the phase diagram. This presumably reflects the presence of ground-state degeneracy, associated with p patterns and thus not connected

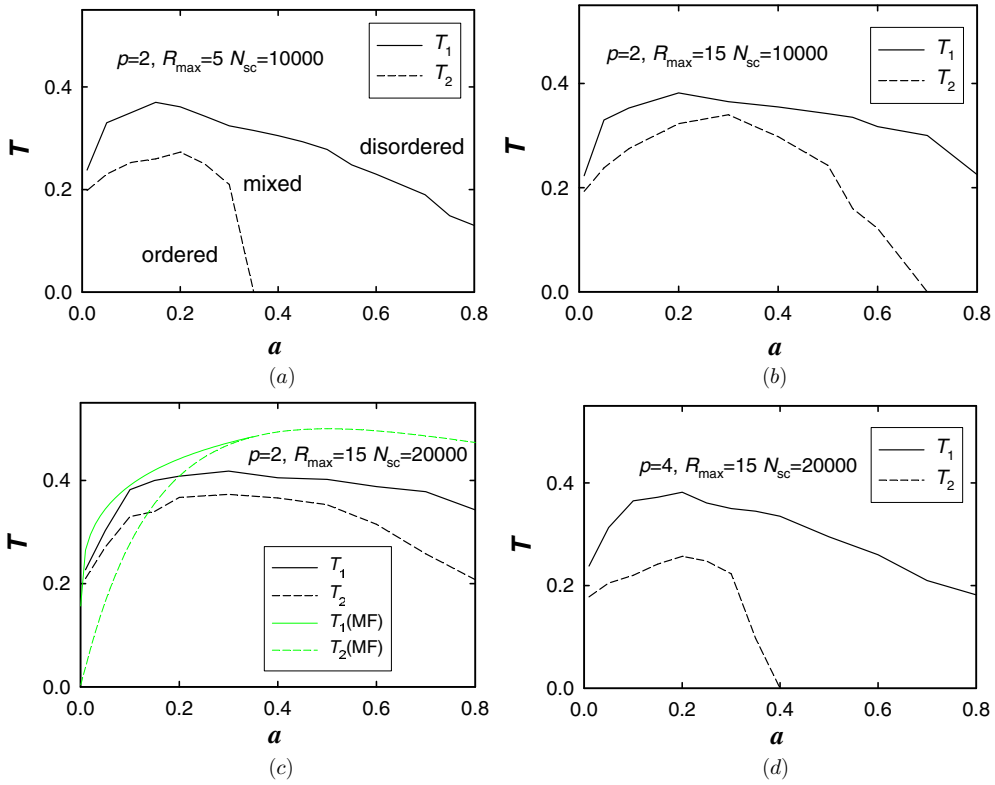

Figure 4. Approximate phase diagrams on the (a, T) plane, obtained from MC calculations for systems on a square lattice of $L = 64$, with parameters (a) $p = 2$, $N_{sc} = 10\,000$, $R_{max} = 5$; (b) $p = 2$, $N_{sc} = 10\,000$, $R_{max} = 15$; (c) $p = 2$, $N_{sc} = 20\,000$, $R_{max} = 15$; and (d) $p = 4$, $N_{sc} = 20\,000$, $R_{max} = 15$. Here T_1 (plotted by solid lines) corresponds to the transition temperature between the disordered phase and the mixed phase, and T_2 (dashed lines) between the ordered phase and the mixed one. For comparison, (c) also shows theoretical curves of T_1 and T_2 for the fully connected (mean-field) system, plotted by thick gray lines.

via the underlying up-down symmetry. As the order parameter becomes larger, however, the power spectrum gradually deviates from the power law at low frequencies. Namely, the frequency range of the power-law behavior is rather limited to mid- to high-frequencies. This trend is more pronounced as the system moves toward more ordered states, shown in figure 5(c).

Apart from deviations from the power law at low frequencies, the system exhibits rather peculiar behavior for short correlation lengths. Looking closely into figures 5(a), (b), and (c), we observe apparent inflection points in the $P(\omega)$ curves when the range is short ($R_{max} = 5$). We stress that the presence of these inflection points is not a computational artifact, for the curves represent average values over many configurations. Such anomalous features were already observed in the system with a small number of connected neurons without shortcuts [7]. It was then suggested that the qualitative behavior depends on how neurons are connected, not just on the connectivity. It now becomes clear that those anomalous features are related to short correlation lengths. Our results further indicate that the power spectrum follows power-law behavior in a wider frequency range as the shortcut range or the correlation length becomes longer.

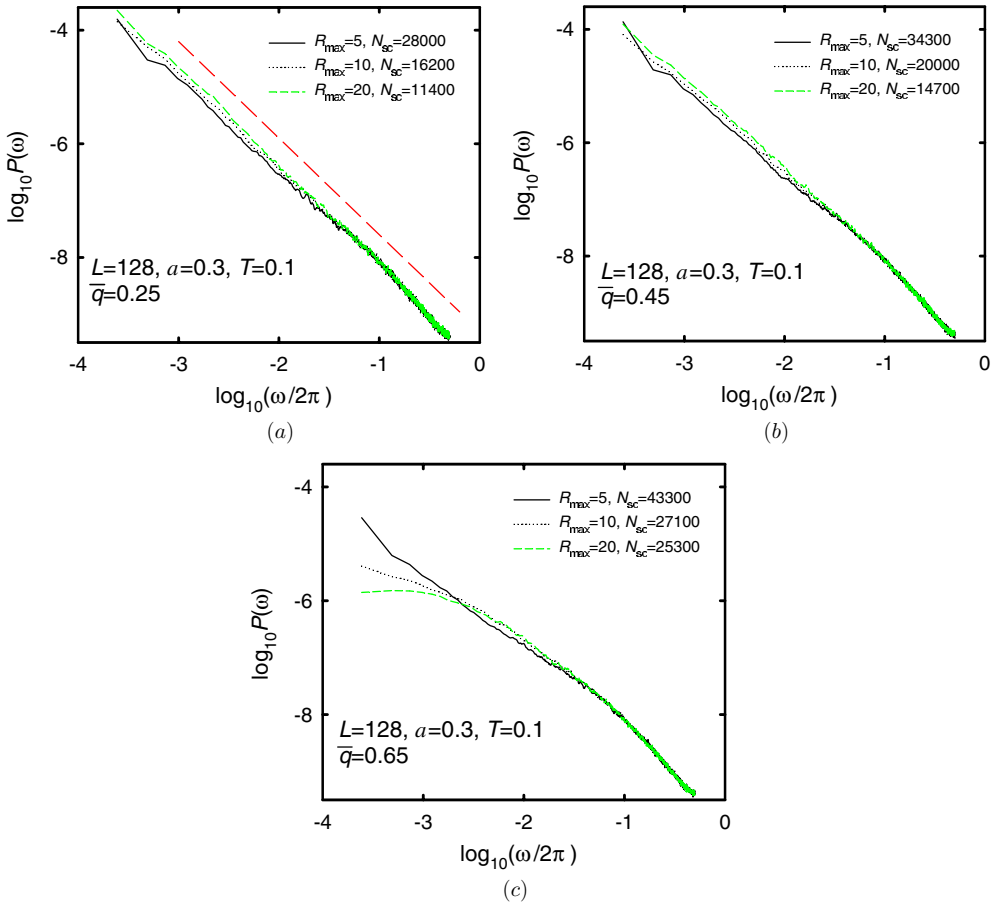

Figure 5. Power spectra for systems on a square lattice of $L = 128$ with three sets of $(R_{\max}, N_{\rm sc})$ shown in the legend, all resulting in the same value of the order parameter: $\bar{q} =$ (*a*) 0.25, (*b*) 0.45, and (*c*) 0.65, corresponding to the mixed phase, ordered phase, and ordered phase, respectively, in the phase diagram. All data have been obtained for $a = 0.3$ and $T = 0.1$. The slope of the straight line in (*a*) is given by -1.7.

It has been already pointed out that spatial and temporal correlations are mutually connected, namely, the distribution of cluster sizes also fits in the power law in the regime where power-law behavior of the power spectrum emerges [7]. We therefore measure the size s of each cluster of memory-unmatched neurons, where a cluster stands for a group of neurons connected as neighbors in the same state. Figure 6 presents the resulting cluster-size distribution $D(s)$ for the same systems as those in figure 5, except the curves for $R_{\max} = 10$ which are omitted for clarity.

As observed in figure 6(*a*), the size distribution in the mixed-phase region fits in the power law $D(s) \sim s^{-\alpha}$ with the exponent $\alpha = 1.8$. Note that the size distribution does not fit well in the power law whenever the power spectrum deviates from power-law behavior in the full range of s; this is manifested in figures 6(*b*) and (*c*), although the distribution $D(s)$ for small values of s may fit in the power law in (b).

It is further observed that the cluster size distribution $D(s)$ has an inflection point when the shortcut range is short ($R_{\max} = 5$) just like the power spectrum $P(\omega)$, again revealing

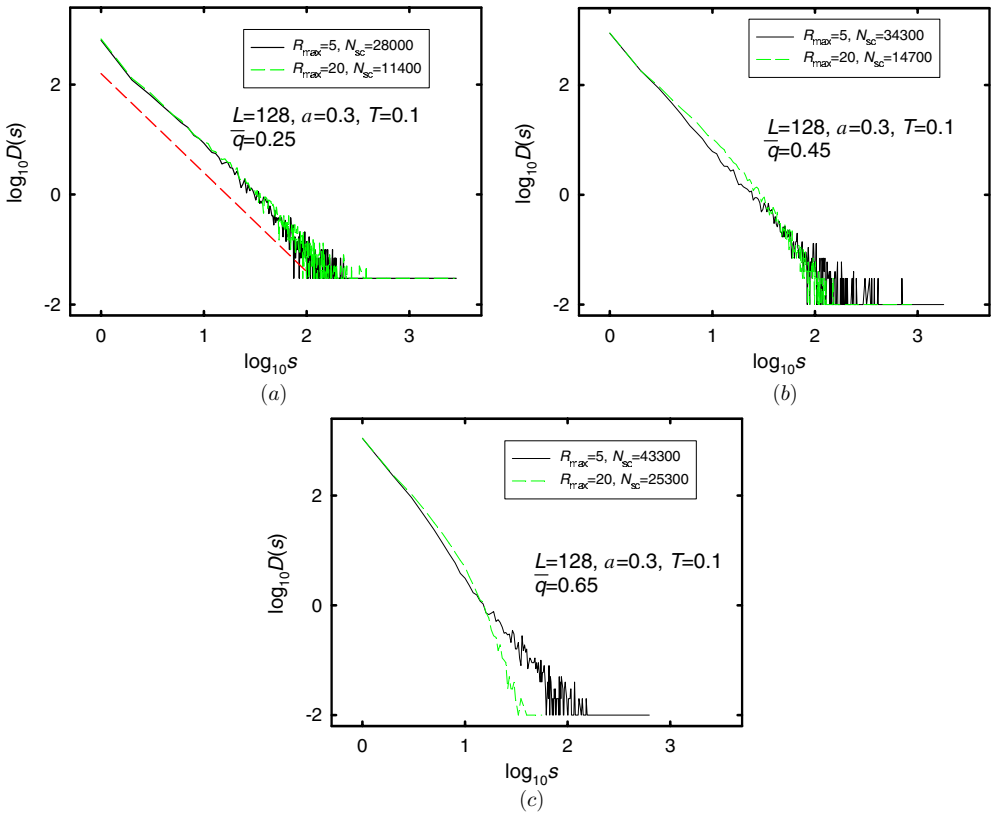

Figure 6. Cluster-size distributions of memory-unmatched neurons for two sets of $(R_{\max}, N_{\rm sc})$ shown in the legends, all corresponding to the data in figure 5. The straight line in (a), drawn for comparison, has the slope -1.8.

the connection between spatial and temporal correlations. This reflects the fact that events involving larger clusters occur rarely, i.e. at lower frequencies while those involving smaller clusters occur more frequently. The frequency or the cluster size, at which the power spectrum or the distribution deviates from the power-law behavior, tends to shift to smaller values for systems with relatively shorter ranges of shortcuts.

Finally, we consider the waiting time t_w, which was defined earlier as the time elapse for a resting neuron to wait for the next firing, and show in figure 7 the wait-time distribution $D(t_w)$, obtained for the same parameters as those in figure 6. The overall shape of $D(t_w)$ appears to depend more or less on the shortcut range $R_{\max}$ as well as the value of the order parameter itself. For example, the inflection point for $R_{\max} = 5$ moves toward higher values of t_w as the order parameter is increased. It is observed that, for longer ranges or $R_{\max} = 20$, $D(t_w)$ appears to fit better in the power law, $D(t_w) \sim t_w^{\beta}$, for t_w larger than the relaxation time $\tau = 5$. The broken line, plotted for comparison, corresponds to the exponent $\beta = 1.7$, which is consistent with observations in central nerve systems and cortex neurons [9, 12]. Our results suggest that neural networks with shortcuts of longer correlation lengths exhibit behaviors following power laws more closely than those of shorter correlation lengths; this apparently supports the small-world architecture in nervous systems, with regard to the power-law behavior.

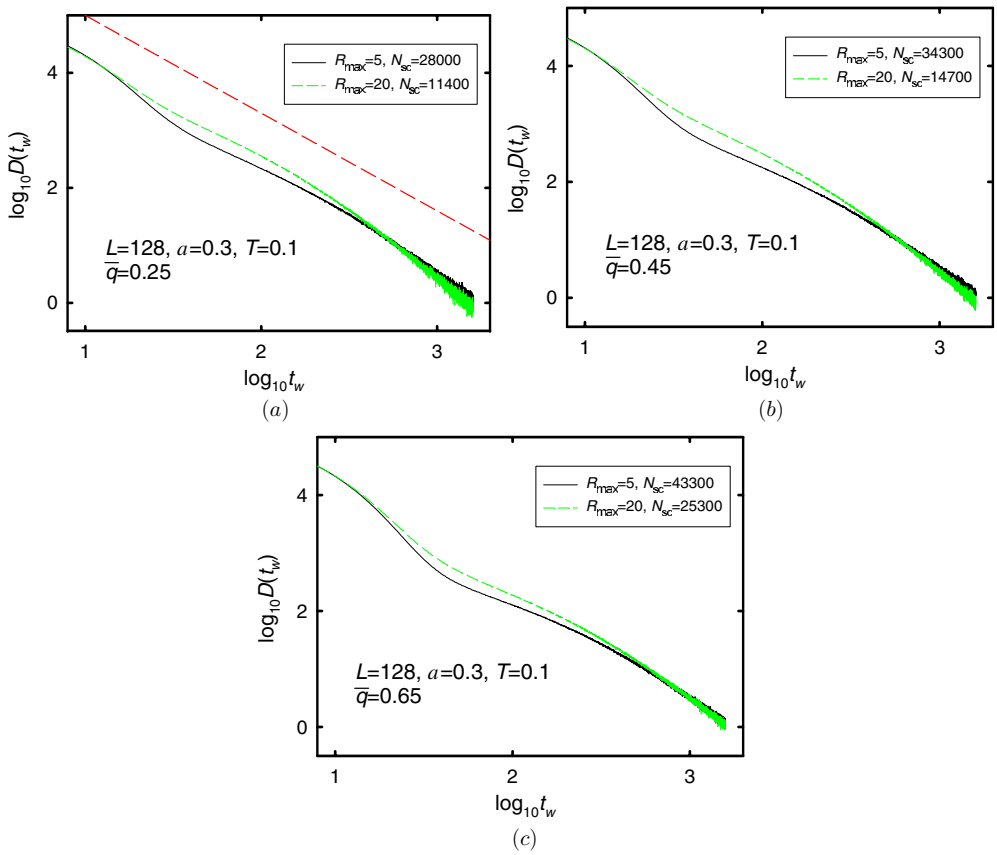

Figure 7. Wait-time distributions of resting neurons for the data in figure 6. The slope of the straight line in (a) is -1.7.

5. Summary

We have studied, via extensive Monte Carlo calculations, the effects of the range of shortcuts in the dynamic model of neural networks. For this purpose, the neurons are placed on a two-dimensional lattice and add shortcuts randomly within some maximum distance, which provides a measure of the correlation length.

It has been observed that the Mattis-state order parameter grows gradually with the shortcut range or the correlation length. When the range is short, the system may be in the multiple-memory state for which mixture of memories is retrieved. We construct the phase diagram on the time ratio versus temperature plane for short/long ranges of shortcuts; the ordered-phase region in general expands with the shortcut range, manifesting the enhancement of memory retrieval with the correlation length. Further, there always appears the mixed phase on the phase diagram, regardless of the time ratio, in contrast with the fully connected neural networks.

The power spectrum of the order parameter at stationarity has been found to have correlations with the cluster size distribution of memory-unmatched sites, both exhibiting different behaviors depending on the shortcut range of the network: for short ranges there appears an inflection point at low frequencies or small cluster sizes. For longer ranges of

shortcuts the inflection point disappears and the power-law behavior is observed in a wide range of frequency or of cluster size, manifesting the role of the correlation length in the small-world network. The wait-time distribution has also been considered and found to follow a power law in the presence of shortcuts with long correlation lengths. These results as to the power-law behavior are apparently suggestive of the small-world architecture in nervous systems exhibiting power-law behavior.

Acknowledgments

BGY thanks to Prof H K Pak for his hospitality during his stay at Pusan National University, in which part of this work has been performed. This work was supported by the Korea Science and Engineering Foundation (KOSEF) Grant funded by the Korea government (MEST) No. R01-2008-000-20025-0 (BGY) and by the National Research Foundation (NRF) through the Basic Science Research Program (grant no. 2009-0080791) (MYC).

References

[1] Watts D J and Strogatz S H 1998 *Nature* **393** 440
Watts D J 1999 *Small Worlds* (Princeton: Princeton University Press)
Watts D J 1999 *Science* **284** 79
Dorogovtsev S N and Mendes J F F 2002 *Adv. Phys.* **51** 1079
[2] Basset D S and Bullmore E 2006 *Neuroscientist* **12** 512
[3] Roerig B and Chen B 2002 *Cereb. Cortex* **12** 187
Roerig B, Chen B and Kao J P Y 2003 *Cereb. Cortex* **13** 350
[4] Sporns O, Tononi G and Edelman G M 2000 *Cereb. Cortex* **10** 127
Laughlin S B and Sejnowski T J 2003 *Science* **301** 1870
Chialvo D R 2004 *Physica* A **340** 756
[5] Bohland J W and Minai A A 2001 *Neurocomputing* **38–40** 489
[6] de Arcangelis L, Perrone-Capano C and Herrmann H J 2006 *Phys. Rev. Lett.* **96** 028107
Pellegrini G L, de Arcangelis L, Herrmann H J and Perrone-Capano C 2007 *Phys. Rev.* E **76** 016107
[7] Choi J, Choi M Y and Yoon B-G 2009 *J. Phys. A: Math. Theor.* **42** 205003
[8] Pritchard W S 1992 *Int. J. Neurosci.* **66** 119
Linkenkaer-Hansen K, Nikouline V V, Palva J M and Ilmoniemi R J 2001 *J. Neurosci.* **21** 1370
Beggs J and Plenz D 2003 *J. Neurosci.* **23** 11167
Freeman W J, Holms M D, West G A and Vanhatalo S 2006 *Clin. Neurophysiol.* **117** 1228
[9] Papa A R R and Da Silva L 1997 *Theory Biosci.* **116** 321
[10] Choi M Y 1988 *Phys. Rev. Lett.* **61** 2809
Choi M Y and Choi M 1990 *Phys. Rev.* A **41** 7062
[11] Hebb D O 1949 *The Organisation of Behaviour* (New York: Wiley)
[12] Gisiger T 2001 *Biol. Rev.* **76** 161